NMR Study of Collective Motions and Bending Rigidity in Multilamellar System of Lipid and Surfactant Bilayers

J. Struppe[a], F. Noack[a], and G. Klose[b]

[a] Universität Stuttgart, Physikalisches Institut Teil 4, Pfaffenwaldring 57, D-70550 Stuttgart
[b] Universität Leipzig, Physikalisches Institut Abteilung BIM, Linnéstr. 5, D-04103 Leipzig

Z. Naturforsch. **52a**, 681–694 (1997); received March 29, 1997

The frequency dependence of the longitudinal proton spin relaxation time T_1 was measured by field-cycling and standard NMR techniques at different temperatures in the liquid crystalline lamellar phases of bilayer systems, composed of lipids, nonionic surfactants, and lipid-surfactant mixtures. We show by our data analysis, comparing various motional models such as layer undulations (LUs) and relaxation by translational diffusion mediated reorientations (TR), that collective layer undulations with their typical $T_1 \sim \nu$ behaviour determine the low frequency T_1 dispersion in both unoriented and glass plate-oriented bilayer systems. The angular dependence of the T_1 dispersion for the oriented bilayer system supports these findings and provides a more critical analysis of the two dimensional self-diffusion than in unoriented samples. The evaluated fitting parameters of the LU model allows, together with the measured second moment of the proton NMR signal for the lipid, calculation of the bending rigidity $\varkappa_c$ for these bilayers at different levels of hydration. The obtained values of $\varkappa_c$ turn out to be too large compared with the literature. However, using recent LU models (B. Halle) which include the obvious couplings between neighbouring bilayers at low Larmor frequencies, the corrected $\varkappa_c$ of the fully hydrated membrane systems are comparable to those obtained from the standard videooptical experiments. Therefore proton spin relaxation measurements at low Larmor frequencies with the field-cycling technique are a suitable means to determine the bending rigidity $\varkappa_c$ of model membrane systems at low hydrations and of systems containing surfactants.

Key words: Proton spin relaxation, field cycling, relaxation dispersion, biological model membrane, membrane undulations, bending rigidity.

1. Problems and Aim

NMR studies of slow collective molecular motions and the related bending rigidity in lyotropic lamellar liquid crystalline phases like lipid and surfactant bilayers are still very controversly discussed. This controversy originates from both different theoretical approaches *and* from the much too restricted available experimental data which are insufficient to give an unambiguous preference. On the one side such motions were originally and still are modeled by 3-dimensional order director fluctuations (ODFs) of *nematic* liquid crystals (LCs) [1–3]. On the other side the modelling was later treated on the basis of 2-dimensional order director fluctuations or layer undulations (LUs) of *smectic*-A LCs under the assumption that no coupling occurs between individual membranes [4, 5]; more recently it was suggested that in multilamellar systems the coupling between the layers is essential for the distribution of undulation modes and hence should be taken into account [6]. Since it took many years to demonstrate clearly the significance of collective motions by NMR relaxation [1, 7, 8], the experimental confirmation of the disputed details is not trivial, particularly in view of the sophisticated NMR techniques used to separate the frequency regimes of collective and non-collective molecular reorientations [9].

Brown et al. [2] performed extensive measurements of ^{1}H, ^{2}H and ^{13}C relaxation times T_1 in various lipid bilayers at standard high Larmor frequencies ν and discussed the results essentially by using the well known square-root dispersion law [1, 10] $T_1(\nu) \sim \nu^{1/2}$ for 3-dimensional ODFs of nematic LCs, which is well-established for numerous nematic mesophases [8] and which under special conditions can also be expected for smectic-A LCs [11]. As his experiments were done only at standard Zeeman fields, i.e. at frequencies from about 4 to 100 MHz where for thermotropic LCs relaxation by ODF was found to be negligible or at least of minor importance [7, 8], Brown's interpretation was strongly disputed by Mar-

Reprint requests to J. Struppe, Dept. of Chemistry & Biochemistry, University of California, 9500 Gilman Drive, La Jolla, California 92093-0359, USA. Fax: (6 19) 5 34-61 74.

0932-0784 / 97 / 1000-0681 $ 06.00 © – Verlag der Zeitschrift für Naturforschung, D-72027 Tübingen

qusee et al. [5] and by Rommel et al. [12] on both theoretical and experimental arguments, namely that smectic LUs and not 3-dimensional ODFs should be considered to describe both the frequency dependence and the absolute order of magnitude of T_1 correctly.

This implies a dispersion law different from the $T_1 \sim \nu^{1/2}$ profile [4, 5], and furthermore the theoretically expected magnitude of a potential relaxation rate by 3-dimensional ODFs is between one and two orders of magnitude higher than seen by the experimental T_1 data. Therefore, the kind of collective molecular motions suggested by Brown et al. cannot explain consistently the available $T_1(\nu)$ measurements [12].

Refining previous calculations of Blinc et al. [4], Marqusee et al. [5] calculated the T_1 relaxation dispersion by thermally activated LUs of uncoupled membranes. It was shown that such a model should lead to a linear dispersion law $T_1 \sim \nu$ within the frequency range of the membrane modes, i.e. between a lower and an upper frequency cut-off. The undulations can be imagined as 2-dimensional fluctuations of the director field, which to a first approximation is assumed to be parallel to the bilayer normal. This linear $T_1(\nu)$ dependence was clearly found by proton NMR fast field-cycling (FC) measurements at low and medium Larmor frequencies for the *lyotropic* lamellar phase of aqueous potassiumlaurate solutions [13] as well as for several high-temperature *thermotropic* smectic-A and smectic-C mesophases [8, 14], whereas the available few experimental results for biological membranes [12] are still less evident or convincing, mainly because other superimposed relaxation processes conceal the full development of the LU contribution to T_1. Similar problems with the model analysis were also encountered for later measurements of the effective transverse relaxation time $T_{2\text{eff}}(\nu')$ [15] as a function of the pulse spacing $\tau = (2\pi\nu')^{-1}$, using the Carr-Purcell-Meiboom-Gill (CPMG) pulse sequence. Nevertheless both the FC and the CPMG data indicate that basically Marqusee's concept is much better suited than the ODF approach.

In recent theoretical papers Halle [6, 16] in principle followed Marqusee's approach (he extends the underlying ansatz for the elastic free energy to the full 3 dimensional case [1]), but introduced refinements by pointing out that the modelling of bilayer undulations involves some subtleties which have been ignored so far in all previous reported studies; in particular he criticized that the coupling between adjacent bilayers was completely neglected. Taking such interactions into account maintains the linear dispersion profile at high frequencies, but decreases the frequency dependence approximately to a characteristic logarithmic behaviour $T_1 \sim \ln[1/N + \nu/\nu_p)]$ below a cut-off frequency ν_p (called patch frequency), which reflects the orientational correlation of N coupled membrane layers, in other words the transition from 2- to 3-dimensional fluctuations. Like any limiting (longest wavelength) undulation mode the cut-off not only decreases the $T_1(\nu)$ slope for $\nu < \nu_p$, but also eliminates the relaxation rate divergence at $\nu \Rightarrow 0$ [10–14]. So in order to distinguish experimentally between Marqusee's theory from Halle's coupled membrane theory (CMT) of spin relaxation one encounters the additional problem to contrast different types of cut-off models with available $T_1(\nu)$ data.

In addition to the collective motions there exist non-collective slow molecular reorientations in membranes, which are also claimed to contribute to the low frequency T_1 relaxation dispersion, namely rotations mediated by translational diffusion on curved surfaces [12, 17, 18]. The influence of such processes on both FC T_1 and CPMG $T_{2\text{eff}}$ measurements of membranes has not been explored in detail up to now, and the similar dispersion profiles expected for collective and non-collective motional models further complicate the interpretation of relaxation data.

This paper presents and analyses new systematic frequency, temperature and concentration dependent FC proton spin relaxation time measurements on various lamellar liquid crystals, namely on: (i) some lipid bilayer systems, (ii) a series of nonionic surfactant bilayers [19], and (iii) bilayers of lipid surfactant mixtures [20]. By such samples it was expected to systematically vary the relative importance of relaxation by collective motions, with the emphasis on *low frequencies* below about $\nu = 1$ MHz, in order to see more details of the $T_1(\nu)$ dispersion profiles than in the case of DMPC (1,2-dimyristoyl-sn-3-phosphatidylcholine), which up to the present is the only biological model membrane studied by FC NMR [12]. We also prepared a mechanically oriented bilayer to investigate the *angular dependence* of the relaxation dispersion for a better separation of the manifold relaxation mechanisms. *Temperature dependent* studies help to disentangle the contributions caused by diffusion and membrane undulations. The study of the *hydration dependence* gives information about the layer couplings and sample preparation effects. Our results suggest a preference of the LU models [5, 16] in contrast to the ODF model

and thus allow to evaluate the bending rigidity $\varkappa_c$ of the bilayers and it's dependence on both the amount of *hydration* and the molecular *lipid geometry*. However, CMT refinements due to the layer couplings are not clearly seen. Our data considerably extend previous studies of $\varkappa_c$ in the literature by other methods [21] and will be compared with theoretical predictions [21, 22].

2. Experimental Methods

2.1. Materials

The lipids DMPC (1,2-dimyristoyl-sn-3-phosphatidylcholine), DPPC (1,2-dipalmitoyl-sn-3-phosphatidylcholine) and DOPC (1,2-dioleoyl-sn-3-phosphatidylcholine) were purchased from SIGMA-ALDICH Chemie, and the lipid POPC (1-palmitoyl-2-oleoyl-sn-3-phosphatidylcholine) from AVANTI-Polar-Lipids. All samples were prepared at different hydrations as shown in Table 1 in the L_α and in the $L_\alpha + H_2O$ phase [23] (2-phase system with free water). We express the hydration in terms of the molar ratio $R_{W/L}$ (with W for water and L for lipid). The transition from the L_α to the $L_\alpha + H_2O$ phase occurs for all studied lipids at approximately $R_{W/L} \cong 20$, where the water layer between adjacent membranes reaches its maximum thickness [24]. For these distinct phases two hydration techniques are necessary due to the two different aspects, namely homogeneous hydration in the L_α-phase and homogeneous distribution of large multilamellar vesicles in the $L_\alpha + H_2O$ phase [25, 26]. Before the hydration the solvent chloroform of the DOPC-$CHCl_3$ solution (as delivered by SIGMA-ALDRICH) had to be removed. The major part of $CHCl_3$ was withdrawn by a soft argon gas flow over the surface of the DOPC-chloroform solution. Then the residual traces of chloroform in DOPC as well as possible residual traces of water in the other lipids were removed in vacuum (10^{-5} mbar) for 2–3 days [27].

The highly hydrated lipid samples in the $L_\alpha + H_2O$ phase were prepared with heavy water (to better separate the lipid from the water signals) by simply mixing the respective amounts of D_2O with the dried lipids. Homogenisation was obtained using standard procedures [25, 26], namely repeatedly vortexing above the main phase transition, i.e. in the liquid crystalline phase [28], followed by freeze-thaw cycles and centrifuging to provide a homogeneous distribution of the size of the large multilamellar vesicles (MLVs) and of the free D_2O between the MLVs in the sample. The samples with water concentrations up to $R_{W/L} = 15$ were hydrated in argon gas atmosphere saturated with D_2O vapour (100% humidity) at a temperature of $\vartheta = 45\,^\circ C$ for 48 to 72 hours in a two chamber NMR glass tube sealed by a teflon plug with an O-ring. The first chamber contains the weighted amount of lipid and the second the necessary D_2O; both are separated by a thin perforated wall to prevent direct contact of the lipid with the liquid D_2O. After hydration the second chamber was removed and the hydration checked by weighing the sample. Finally the mixtures were transferred under argon gas atmosphere into 10 mm diameter NMR glass tubes using a centrifuge, then frozen to seal them under soft vacuum (0.3 bar).

The surfactants C_nE_m (*m*-ethyleneglycol-*n*-alkylether), namely $C_{12}E_3$, $C_{12}E_4$, $C_{12}E_5$, $C_{12}E_6$, $C_{10}E_4$ and $C_{16}E_4$ were purchased from FLUKA Chemie and directly filled into the NMR sample tube. Then the

Table 1. Lyotropic liquid crystalline systems studied in this paper. The ratio between the water and the lipid or surfactant is given by two quantities: the molar ratio $R_{W/L}$ and the weight percent of ^2H_2O in the mixture. The lipid-surfactant mixtures are characterized by their molar weight, and by the mole ratio of the surfactant $C_{12}E_4$ (S) to the phospholipid POPC (L).

Phospholipid	Molar weight *g*/Mole	Molar ratio $R_{W/L}$	Weight percent %
DMPC	677.9	15	30.7
DMPC		40	54.2
DPPC	734.0	40	52.2
POPC	760.1	10	20.9
POPC		20	34.5
POPC		40	51.3
DOPC	786.1	40	50.5
Surfactant	**Molar weight *g*/Mole**	**Molar ratio $R_{W/S}$**	**Weight percent %**
$C_{12}E_3$	318.5	10	38.6
$C_{12}E_4$	362.6	10	35.6
$C_{12}E_4$		40	69.0
$C_{12}E_5$	406.6	10	33.0
$C_{12}E_6$	450.7	10	30.8
$C_{10}E_4$	334.5	10	37.4
$C_{16}E_4$	418.7	10	32.4
Surfactant/ lipid mixture $R_{S/L}$	**Molar weight *g*/Mole**	**Molar ratio $R_{W/(L+S)}$**	**Weight percent %**
1	563.8	7	20
1		19	40
1		42	60
4	442.1	5	18
4		13	37
4		31	57

desired amount of D_2O was added and homogeneous mixing obtained by stirring the samples before sealing as described above. The influence of surfactants on lipids was studied for two lipid (L) surfactant (S) mixtures, which were prepared with POPC and $C_{12}E_4$ [29, 30] namely for the molar ratios $R_{S/L}=1$ and 4. The $R_{S/L}=1$ mixture was obtained by solving both components in methanol followed by the solvent removing technique described above. The $R_{S/L}=4$ mixture was obtained by directly mixing the compounds without the need of additional organic solvent to obtain homogeneous mixing. The hydrations $R_{W/(S+L)}$ for the prepared mixtures as listed in Table 1 were achieved with the same technique used for the lipid samples.

The oriented DMPC samples were prepared between 70 μm thick, 25 mm long, and 4, 6, and 8 mm broad borosilicate glass plates, in order to obtain optimum filling factor. Such borosilicate glass plates were provided by Marienfeld AG. We followed the preparation technique proposed by Powers and Clark [31] with the improvements of Prosser et al. [32] to get better orientation and sample filling. Applying this technique we obtained 250 mg oriented DMPC (≈ 78 glass plates in the NMR sample tube; 10 mm diameter) which was enough to provide a good NMR signal. The sample was hydrated in argon gas atmosphere saturated with D_2O vapour at $\vartheta=50\,^{\circ}C$ for 48 to 72 hours and then the hydration was checked by weighing the sample. We achieved a maximum hydration $R_{W/L}\approx 11\pm 1$, which mean about 3 moles D_2O per mol lipid less than reported in literature [33, 34]. Higher water concentrations can only be achieved by pipetting water directly to the sample [32]. The quality of the alignment was checked by polarisation microscopy and ^{31}P NMR spectra [15].

2.2. Methods

The proton $T_1(\nu)$ field-cycling measurements were performed in Stuttgart on two home-built field-cycling spectrometers by standard techniques [7, 35] in the frequency range $100\,Hz\leq\nu\leq 33\,MHz$ and temperature range $0\leq\vartheta\leq 70\,^{\circ}C$. Both instruments need sample volumes of about 1 cm^3. Estimated from the experimental scatter the accuracy of the presented T_1 data is better than $\pm 10\%$. Temperature calibration and determination of its gradient was achieved with errors of about $\pm 0.2\,^{\circ}C$ and $0.1\,^{\circ}C/cm$, respectively, by the change of the free induction decay (FID) following a $\pi/2$ pulse of simple thermotropic LC's like e.g. the 4-*n*-alkyl-4′-cyanobiphenyls (*n*CBs) 5CB and 8CB [27]. Over signal decays of typically up to two time constants, the spin relaxation process was observed to be single exponential. The 100 MHz T_1 measurements were made on the same samples in Leipzig by means of a Bruker MSL 100 spectrometer, which was also used to determine the 2nd moment (M_2) of the line widths following the procedure of Bloom et al. [36]. The samples were stored in a refrigerator and proved stable for several months. For the studies of the angular dependence the aligned samples could be rotated in the NMR probe by the desired angle with an accuracy of ± 2 deg. In order to examine the influence of the surfactant on the mesoscopic lamellar structure of the lipid we made use of electron microscopy freeze-etch replicas [33] for some lipid surfactant mixtures.

3. Results

The following figures illustrate typical T_1 dispersion profiles for some lipids and surfactant systems under selected special conditions, namely at different hydrations and temperatures. In particular these diagrams show *four* aspects on which our quantitative model analysis of the layer undulations will be based: The general parallels with previous data for thermotropic smectic LC's, the strong distinctions between lipids and surfactants systems at low Larmor frequencies, the rather different effects due to changing hydrations and temperature at low and high frequencies, and finally the comparison of the individual lipids and surfactants with the LS mixtures. In addition, we consider the distinction between oriented and non-oriented bilayers to improve the separation of different dispersion regimes.

In order to illustrate some common features in the T_1-dispersions of liquid crystalline systems, Fig. 1 presents selected $T_1(\nu)$ measurements for POPC in the $L_\alpha+H_2O$ phase ($R_{W/L}=40$) and for $C_{12}E_3$ in the L_α phase ($R_{W/S}=10$) at $\vartheta=30\,^{\circ}C$, and compares these results with typical T_1 dispersions of thermotropic liquid crystals in the nematic phase (5CB, N, broken line) and in the smectic phase (8CB, Sm, dotted line) [37, 38] at the same temperature. It can be seen that in all cases the relaxation dispersion is separable into (at least) two frequency ranges; the transition from the first to the second region occurs between 10 kHz and 100 kHz and depends on properties of the system

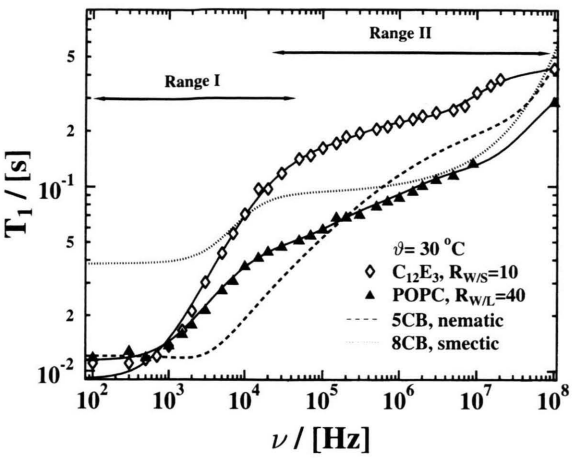

Fig. 1. Larmor frequency dependence of the longitudinal proton spin relaxation time T_1 for the lyotropic liquid crystalline POPC/^2H_2O system in the water rich liquid crystalline lamellar phase ($L_\alpha + H_2O$-phase) and for $C_{12}E_3$ in the liquid crystalline lamellar phase (L_α-phase). These experimental results are compared with previous results for thermotropic liquid crystals, namely 5CB (nematic) and 8CB (smectic A). The solid lines represents fits of the motional model to the experimental data for both lyotropic systems. The models contain three underlying contributions, the collective molecular motions (layer undulations) and the two individual molecular motions, translational and rotational diffusion. From the diagram one can distinguish at least two characteristic relaxation regimes: range I, which includes the low frequency plateau and the first dispersion step, and range II, which comprises the subsequent flatter dispersion in the medium frequency range between approximately 10 and 500 kHz, and the increasing T_1 dispersion in the high frequency region above several MHz. The transition between the two regions lies between 10 kHz and 100 kHz, depending on the system studied.

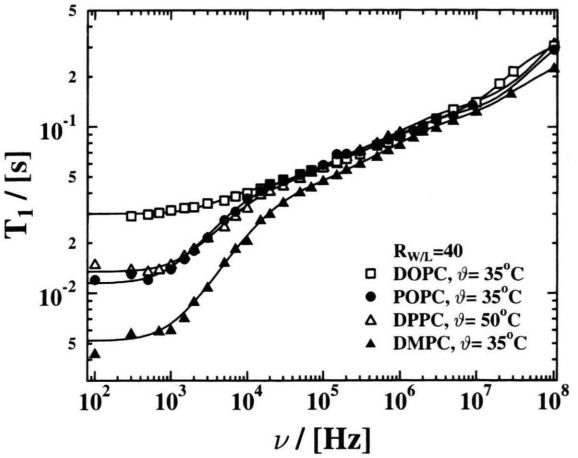

Fig. 2. Frequency dependence of the proton T_1 for the four phospholipid systems DOPC, POPC, DPPC, and DMPC, studied at the same hydration in the $L_\alpha + H_2O$-phase. The solid lines represents fits of the motional models to the experimental data as described in the text with the parameters listed in Table 2. Note that in order to reach the liquid crystalline phase, the temperature for DPPC was somewhat higher than for the other lipids. The experimental error is smaller than the symbol size; within these error limits, the onset of the first dispersion step is the same for all these lipid systems with the exception of DOPC, where no dispersion step is clearly visible.

studied: Range I comprises a low-frequency plateau followed by a strong first dispersion step with $T_1 \sim \nu^\alpha$, where α is between 1/2 and 1. The step size is the difference of T_1 between the low-frequency plateau ($\nu \leq 1$ kHz) and the onset of range II, where at medium frequencies another $T_1(\nu)$ plateau is approached or fully developed, followed by a shallow but clearly seen second dispersion step. This behaviour is most conveniently observed for 8CB and $C_{12}E_3$, whereas due to an overlap of the two ranges the separation is less evident for the other examples. Our new results are essentially in accordance with our previous studies on DMPC [12] and with proton relaxation data reported for range II by other groups [2, 9]. Figure 1 also reveals a remarkable feature of lyotropics which cannot be seen by conventional high-field NMR: In range I the lipids characteristically exhibit a rather small dispersion step in contrast to the surfactants, where as a rule this step is rather strong [12, 27].

Figure 2 compares the $T_1(\nu)$ results for the lipids DOPC, POPC, DPPC, and DMPC in the $L_\alpha + H_2O$-phase with a hydration $R_{W/L} = 40$; due to the high main phase transition temperature of 42 °C the measurements for DPPC had to be performed at a somewhat higher sample temperature (50 °C) than for the other systems (35 °C). As in Fig. 1 one has two distinct dispersion ranges. In region I the $T_1(\nu)$ step is found to decrease in the order DMPC ⇒ POPC/DPPC ⇒ DOPC, i.e. with increasing fatty acid chain length (DMPC ⇒ DPPC) and increasing number of unsaturated fatty acid chains (DMPC ⇒ POPC ⇒ DOPC) of the lipids. As a consequence only a rather tiny dispersion step remains visible for DOPC. The onset of the T_1 frequency dependence in range I is the same for all lipids within the error limits, namely at approximately $\nu = 1$ kHz, whereas the low frequency plateaus greatly differ by almost a factor of 5. E.g. $T_1(\nu \cong 0)$ of DMPC is half the value of $T_1(\nu \cong 0)$ for DPPC and POPC. In contrast to this finding the dispersion profiles for DMPC, DPPC and POPC are almost identical in range II ($\nu > 30$ kHz), only DMPC reveals a

non-negligible vertical shift by about 25%. This indicates that here the fatty acid chain length as well as the number of unsaturated fatty acid chains cannot play a significant role for the underlying relaxation process. The magnitude of effects caused by temperature variations will be explained separately.

Figure 3 shows the results for the surfactant $C_{12}E_4$ in the L_α-phase at two hydrations ($R_{W/S}=10$ and 40) and two temperatures ($\vartheta=30$ and 50 °C) to demonstrate the strongly different T_1 variations in ranges I and II, respectively. It is clearly seen that at low ν's (< 5 kHz) the dispersion profile, i.e. both the T_1 plateau and the subsequent $T_1(\nu)$ slope, is very sensitive to changes of the hydration ratio $R_{W/S}$ but insensitive to temperature changes, whereas at high ν's (> 2 MHz) the opposite is true; in the transition region from I to II both effects mix in a complex way. The low-frequency plateau and the beginning of the low-frequency dispersion step decrease at higher hydrations. A qualitatively similar behaviour was observed for all surfactants and lipids studied [27], though in the latter case, essentially due to the much smaller $T_1(\nu)$ step in range I, the disentanglement of the dependencies on R and ϑ is less straigthforward than for the surfactants.

As an example, Fig. 4 gives $T_1(\nu)$ data for the lipid DMPC at different hydrations ($R_{W/L}=15$ and 40) and temperatures ($\vartheta=30$, 35 and 50 °C). The comparison with Fig. 3 reveals qualitative parallels between the dispersion profiles like the weak hydration and strong temperature effects in range II, but also apparent distinctions like a small, non-vanishing temperature dependence in range I. Note that there exist plot crossing points in both diagrams which follow from the different $T_1(R)$ and $T_1(\vartheta)$ shifts in range I and II; they mark frequencies where the temperature effect is compensated by an inverse hydration effect. Furthermore, lipid surfactant mixtures (Fig. 5, POPC-$C_{12}E_4$, L_α-Phase) illustrate the transition from the typical T_1 characteristics of lipids to the peculiar features of surfactants with increasing $R_{S/L}$ ratio: E.g. the $T_1(\nu)$ profile of the $R_{S/L}=1$ mixture with the small dispersion step in range I is similar to the one of the pure POPC sample, whereas the $R_{S/L}=4$ mixture approaches the $T_1(\nu)$ slope of the pure $C_{12}E_4$ membranes at comparable hydrations.

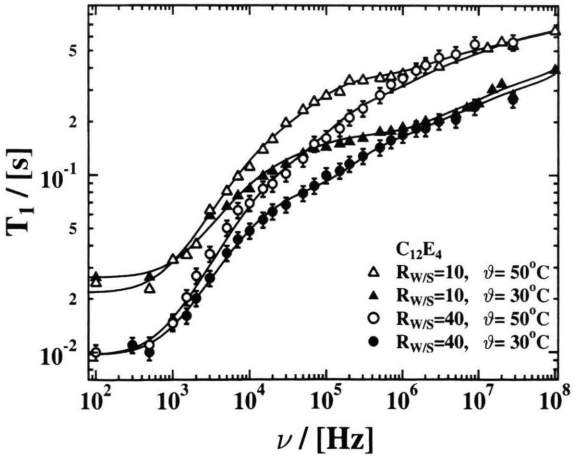

Fig. 3. Frequency dependent T_1 data for the surfactant $C_{12}E_4$ studied at two different hydrations and two different temperatures ($\vartheta=30$ and 50 °C). Range I is mainly determined by the changing hydration and range II by the temperature variation. Both samples are in the liquid crystalline L_α-phase. The solid lines are fits to the models which are described in the text using the parameters given in Table 2.

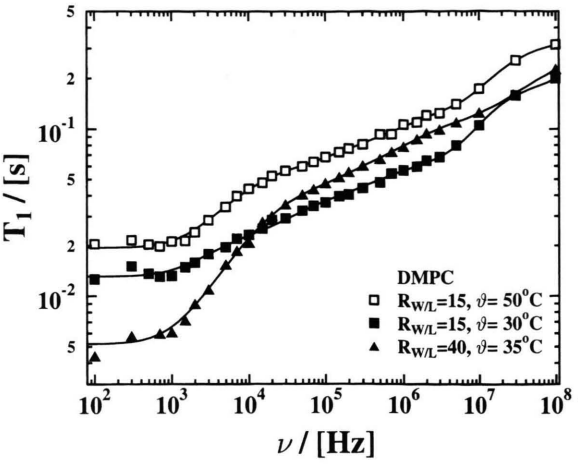

Fig. 4. $T_1(\nu)$ data for DMPC in the L_α ($R_{W/L}=15$) and in the $L_\alpha+H_2O$-phase at the temperatures shown. Note that the T_1 dispersion slopes for 30 and 35 °C cross each other at the end of range I, where the temperature dependence begins to dominate the relaxation dispersion, in contrast to range I where the hydration dominates the shape of the T_1 dispersion. As shown by comparing the 50 °C and 30 °C data, the dispersion step in range I increases with increasing temperature due to the stronger influence of the temperature in range II and its considerable weaker influence in range I.

For all studied samples one generally obtains only a small or even a vanishing temperature dependence of the T_1 dispersion in range I, but a strong variation in range II. The magnitude of such $T_1(\vartheta)$ changes in range I becomes smaller with increasing dispersion step from I to II, which is controlled by the amount of hydration. These findings indicate that in most cases there exists a non-negligible overlap of the two

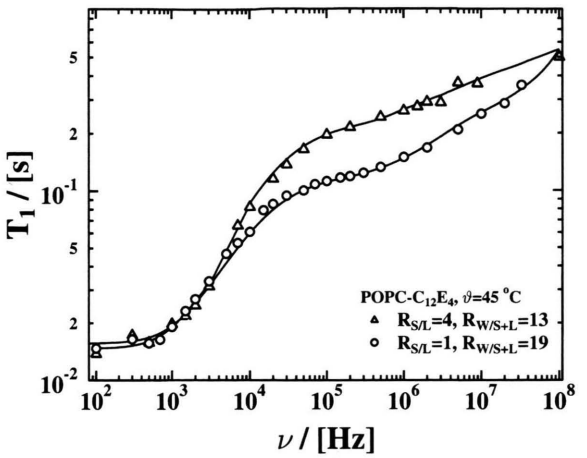

Fig. 5. $T_1(\nu)$ results characteristic for two lipid-surfactant mixtures in the L_α-phase for different molar ratios $R_{S/L}=4$ and $R_{S/L}=1$. The transition from the relaxation characteristics of the lipids to the surfactants can be seen clearly. The solid lines are fits to models described in the text using the parameters listed in Table 2.

regimes, though evidently both ranges reflect totally distinct *dominant* relaxation mechanisms, and thus parallels to previous NMR FC results reported for thermotropic LCs [8]. The basic separation is further supported by T_1 measurements on oriented samples, which show that the macroscopic alignment of the director axis relative to the Zeeman field by an angle Δ considerably changes the dispersion profiles at low and medium, but not at high frequencies. Figure 8 illustrates some results for DMPC at selected angles between $\Delta=0°$, 30°, 50° and 90°. E.g. at $\nu=1$ kHz one has $T_1(0°)/T_1(90°)=3$, whereas for $\nu>5$ MHz this ratio is near 1. Hence the quantitative model of the proton spin relaxation time must explain the systematically different frequency, temperature, hydration and angular dependences observed in range I and II for the numerous studied lamellar systems. In the following we compare our data with both Marqusee's and the CMT predictions on LUs, in combination with additional standard relaxation contributions by non-collective molecular motions.

4. Theory and Discussion

4.1. Relaxation Models

Proton spin relaxation in liquid crystalline systems is described by the theoretical framework of the Redfield formalism in numerous papers, which have recently been summarized in the book of Dong [39]. Under the assumptions of fast magnetization transfer between different kinds of dipolar coupled protons on a LC molecule and sufficiently short correlation times, which are fulfilled in the present experiments, the spin relaxation function is expected single exponential as observed experimentally. In this work we make use of the theory in the notation given previously by Struppe et al. [38] in order to discuss field-cycling relaxation dispersion studies in thermotropic nematic mesophases, however with some minor changes more appropriate in the present case. Individual T_1 models of different molecular reorientation processes are usually expressed by their specific *spectral densities* $J^{(p)}{}_M(p\nu, \Delta)$ in the laboratory frame, where $p=1, 2$, and the index M refers to the considered kind of motion. The total relaxation rate follows by the summation overall possible statistically independent contributions M, i.e.

$$1/T_1(\nu, \Delta) \equiv R_1(\nu, \Delta) = \sum R_{1M}(\nu, \Delta) \tag{1a}$$

$$= \frac{9}{8}\left(\frac{\mu_0 \gamma^2 h}{8\pi^2}\right) \sum_M^2 (J^{(1)}{}_M(\nu, \Delta) + J^{(2)}{}_M(2\nu, \Delta)),$$

where $\nu=\gamma B/(2\pi)\equiv\omega/2\pi$ means the proton Larmor frequency in the Zeeman field $B=|\mathbf{B}|$ and Δ is the angle between this field $\mathbf{B}$ and the LC director $\mathbf{n}$; μ_0, γ, h are the magnetic vacuum permeability, the magnetogyric ratio of protons and Planck's constant, respectively. The factor $Z=(9/8)(\mu_0\gamma^2 h/8\pi^2)^2 = 6.408\cdot10^{-49}\,\mathrm{m^6\,s^{-2}}$ scales the spectral densities $J^{(p)}$ for dipolar spin interactions. As in [38], we use Abragam's notation [40, 41] of the $J^{(p)}$'s with $p=1$ and 2. For uniaxial symmetry these lab frame spectral densities $J^{(p)}{}_M(p\nu, \Delta)$ can be related by model independent transformations $f_{pq}(\Delta)$ [39, 41] to more convenient, not Δ dependent spectral densities $J^{(q)}(p\nu)$ in the director frame with $q=0, 1, 2$, which have been reported in the literature for many molecular processes in LCs. In order to obtain the model relations for unoriented samples, the $J^{(p)}{}_M(p\nu, \Delta)$ must be averaged over all possible orientations according to [41]

$$\langle J^{(p)}{}_M(p\nu)\rangle = \int_0^\pi \sum_{q=0}^2 f_{pq}(\Delta)\, J^{(q)}{}_M(p\nu)\, \sin(\Delta)\, \mathrm{d}\Delta. \tag{1b}$$

Available models $J^{(p)}{}_M$ reflect both the different *geometrical conditions* of unlike mesophase structures, like e.g. 2-dimensional LUs [5] or 3-dimensional ODFs [10], and the different *energetic constraints* on the anisotropic translational and rotational reorienta-

tions by anisotropic hindering potentials, like e.g. diffusion in a plane or rotation on a cone. In lamellar lyotropics, surface effects may play an important role [12, 17, 18].

Unlike deuteron relaxation studies, proton T_1 measurements reveal in addition to the spectral densities of molecular rotations also effects originating from translational diffusion of the spins. As a consequence, four kinds of relaxation mechanisms M have been suggested to determine the proton $T_1(\nu, \Delta)$ data in lamellar LC's namely [12]: **L**ayer **u**ndulations (LU), **r**otational **d**iffusion (Rot), translational **s**elf-**d**iffusion (SD), and **r**otations **m**ediated by **t**ranslational self-**d**iffusion (RMTD). For simple geometries (e.g. spins on spherical surfaces) the RMTD model simplifies to the more familiar so-called **r**otations induced by **t**ranslations (TR) process [18, 42, 43]. The related spectral densities differ more or less by their characteristic Larmor frequency, temperature and angular dependences, so that they can be separated provided sufficient and accurate experimental T_1 data are available. In this study we will be mainly concerned with the assignment of the T_1 dispersion at low ν's, where, as expected by previous studies, *slow* motions like LU and RMTD dominate the overall relaxation rate. Equations (2)–(5) summarize the model expressions and parameters used in the $T_1(\nu)$ analysis of Figures 1–4.

Following Marqusee et al. [4, 5], the layer undulation terms $J^{(q)}{}_{LU}$ give above a low frequency cut-off ν_{CL} of the LU modes a linear dispersion law according to

$$J^{(1)}{}_{LU}(\nu) = A_{LU}(2\pi\nu)^{-1}[(2/\pi)\arctan(\nu/\nu_{CL})], \quad (2a)$$

$$J^{(2)}{}_{LU}(\nu) \cong 0, \quad (2b)$$

which for ν/ν_{CL} leads to an arctan cut-off with a plateau determined by the frequency ν_{CL} and the spectral density amplitude

$$A_{LU} = (k_B T M_2)/(8\kappa_c Z), \quad (2c)$$

where $M_2 \equiv (4\pi^2)\langle \Delta\nu^2 \rangle$ is the time-averaged 2nd moment of the proton line [40]. Halle's [6] original extension took into account couplings between N interacting layers in the *fast* diffusion limit, i.e. when the lateral self-diffusion in the membrane is much faster than the collective LU motions and hydrodynamic effects of the water molecules between the layers can be neglected. The coupling entails significant changes $J^{(1)}{}_{LU}(\nu)$: First, the arctan cut-off profile is replaced by the much shallower logarithmic behaviour

$$J^{(1)}{}_{LU}(\nu) = A_{LU}(2\pi\nu_p)^{-1} \ln[(1+\nu/\nu_p)/(1/N+\nu/\nu_p)] \quad (3)$$

near the so-called patch frequency $\nu_p = D_\perp/2\xi^2$. This frequency reflects the lateral self-diffusion constant $D_\perp$ of the membrane (i.e. $\perp$ to the director **n**), and the orientational correlation or patch length ξ. By Eq. (3) $T_1(\nu)$ depends not only on the characteristic frequency ν_p, but also on the layer number N. Halle's LU model describes a transition from an asymptotic linear high-frequency dispersion like in (2a), to a logarithmic low-frequency profile. The difference from (2a) becomes most pronounced in the limit $N=1$, where the coupling no longer exists and ln 1 vanishes. Second, for $N>1$ the linear regime spreads towards lower frequencies compared with the arctan cut-off, which is important since theoretical estimations of ν_p [6] predict rather large values above 10^6 Hz. This is illustrated by Fig. 6 for several values of N with identical A_{LU} and putting $\nu_{CL} = \nu_p$ to allow a convenient comparison of the arctan and log expression. So in the linear regime, (2a) and (3) cannot be discriminated but outside the linear regime the distinctions are easy to demonstrate. In a later work, Halle [16] also considered the mathematically more cumbersome *slow* diffusion limit (which is more appropriate for the lipid systems studied), where the lateral self-diffusion is

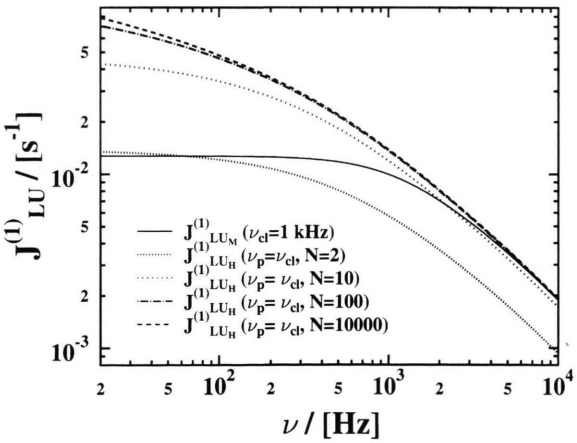

Fig. 6. Larmor frequency dependence of the spectral densities $J^{(1)}$ for layer undulations in the low frequency mode cut-off regime of Halle's and Marqusee's model. Marqusee's model, which is indicated by the subscript M and neglects layer couplings, shows the arctan behaviour (solid line). Halle's model, which is indicated by the subscript H and is the simple coupling model, gives a logarithmic cut off behaviour, for various numbers N of coupled layers shown in the figure.

much slower than collective molecular motions and the hydrodynamics of the water layers should not be neglected. In this case $J^{(1)}{}_{LU}(\nu)$ becomes a complicated integral as a function of parameters for the coupling (σ) and the relative speed of diffusion (δ). By numeric integrations he essentially showed that for high ν's the linear dispersion law approximately persists, however, with a considerably increased spectral density amplitude ($A^*_{LU} \cong 3.4\, A_{LU}$). The factor 3.4 is obtained by numerical evaluation of equation 8.6 in [16] with $\alpha = 12$, $\delta = 0.25$, $N = 10^4$, $\pi(\xi_k/q)^2 = 10^4$ and $\sigma = 0.01$ to 0.2 (the variables are explained elsewhere [16]) and fitting to this result the simple linear LU model. Variations of δ provide for a fixed value of ν_p another critical model parameter to spread the linear $T_1(\nu)$ profile to still lower Larmor frequencies, but the shallow log-like $T_1(\nu)$ profile at low ν's is roughly maintained [16].

The experimental confirmation of Halle's CMT concept is complicated by the circumstance that in lamellar systems hindered diffusion along curved lamellar surfaces may cause various RMTD relaxation mechanisms with dispersion profiles similar to LU processes, namely by spectral densities of the asymptotic forms $J^{(1)}(\nu) \sim \nu^{-\alpha}$, where the exponent α ($0.5 \leq \alpha < 2$) depends on the distribution of curvatures and on details of the molecular reorientation [18, 42, 43]. To distinguish the two types of motions by model fits, simplifying geometrical restrictions are needed. Essentially based on electron microscopic freeze-etch replicas [27, 33] and on the work of Heaton et al. [26], which typically exhibit local spherical curvatures with radii R in the μm range, we considered the simple Debye-type TR spectral densities [42]

$$J^{(q)}{}_{TR}(p\,\nu) = A_{TR}\, p^2\, [\tau_{TR}/(1 + (2\pi p \nu \tau_{TR}{}^2)] \qquad (4a)$$

with

$$A_{TR} = 4\,\zeta_{surf}\, M_2/(15\,Z)\,, \qquad (4b)$$

$$\tau_{TR} = R^2/(6\,D_\perp)\,. \qquad (4c)$$

These relations, where $\zeta_{surf} = A_C/A_L$ denotes the ratio between the curved and the total lamellar surface and $D_\perp$ means the lateral diffusion constant of the lipid or surfactant molecules, were originally reported by Žumer et al. [42] and later extended by Rommel et al. [12] to lipid membranes. The main distinctions between (3) and (4) are on the one hand the stronger T_1 dispersion by (4a), and on the other hand the expected much stronger temperature dependence of the Debye term compared to possible changes of both the ln or arctan law in range II. This follows from the simple circumstance that in this regime $J^{(q)}{}_{LU}(\nu)$ becomes approximately independent on ν_p or ν_{LC}, whereas $J^{(q)}{}_{TR}(\nu)$ strongly reflects variations of $\tau_{TR}(\vartheta)$.

The high-frequency Rot and SD relaxation processes are less disputed because of extensive available measurements by standard NMR spectrometers [9, 39], and only rather fine details of such models are still not satisfactorily solved. We make use of the involved spectral densities with some simplifications to extend the model fits consistently to our data in the upper dispersion range, where the LU and RMTD models are superimposed by the established contributions for anisotropic translational self-diffusion (SD) and rotational reorientations (Rot) [39].

The translational self-diffusion terms $J^{(q)}{}_{SD}(p\,\nu)$ were first reported for layered systems by Vilfan et al. [44] as complicated integral functions $T^{(q)}$ in the form

$$J^{(q)}{}_{SD}(p\,\nu) = A_{SD}\, \tau_{SD\perp}\, T^{(q)}(p\,\nu, \tau_{SD\perp}, \alpha, \eta_{SD}) \qquad (5)$$

with 4 model parameters: the amplitude $A_{SD} = (16\,\pi n)/(45\,d^3)$, the correlation time $\tau_{SD\perp} = \langle r_\perp^2 \rangle / 4\,D_\perp$, the jump width ratio $\alpha = \langle r_\perp^2 \rangle / d^2$, and the diffusion anisotropy $\eta_{SD} = D_\parallel / D_\perp$. Using MAPLE V and results reported by Sebastiao [45], we calculated the $T^{(q)}$'s numerically [27, 38, 44] for the considered geometries, which depend on the length/diameter ratio of the rod like molecules, the proton spin density n, the average jump width $\langle r^2 \rangle$, and the self-diffusion constants D_i parallel ($\parallel$) and perpendicular ($\perp$) to the LC director, respectively. For not too small values of the motional anisotropy, i.e. $0.3 < \eta_{SD} < 5$, the cumbersome evaluation of (5) was simplified by using an anisotropic approximation given by Torrey [44, 46]. The standard expression for the spectral densities $J^{(q)}{}_{Rot}(p\,\nu)$ of rotating ellipsoidal molecules in an anisotropic environment is that given by Nordio et al. [39, 47], which can be approximately written [27] in a form similar to (5):

$$J^{(q)}{}_{Rot}(p\,\nu) = A_{Rot}\, \tau_{R\perp}\, R^{(q)}(p\,\nu, \tau_{R\perp}, \eta_{Rot})\,, \qquad (6a)$$

where the $R^{(q)}$'s are large sums of Debye-terms depending on the LC order parameter, the rotational correlation time $\tau_{R\perp}$ about the short ellipsoid axis, and the rotational anisotropy $\eta_{Rot} = \tau_{R\perp}/\tau_{R\parallel}$. This means 3 model parameters: The amplitude A_{Rot}, one reorientation time $\tau_{R\perp}$, and the ratio η_{Rot}. Equation (6a) was evaluated numerically by means of MAPLE V. To simplify the procedure, we sometimes also tried for the non-oriented samples, in replacement of (6a), the simpler Woessner approach for sym-

metrical ellipsoid rotations in an isotropic environment [48], which in the same notation leads to a sum of only three Debye-terms with amplitudes A_i:

$$J^{(q)}(p\nu) = q^2 [A_{R\parallel}\tau_{R\parallel}/(1+(2\pi p\nu\tau_{R\parallel})^2 + A_{R\perp}\tau_{R\perp}/(1+(2\pi p\nu\tau_{R\perp})^2 + A_{IR}\tau_{IR}] . \quad (6b)$$

The A_i's are determined by the average spin pair orientations and separations on the ellipsoid, and τ_{IR} takes into account internal pair rotations on the molecule. In the present case such an approximation is justified in view of our restricted high-field range, and the intrinsic averaging of unlike proton positions in the NMR spin signal. Except that (6b) does not allow to describe the angular dependence $T_1(\Delta)$ due to the assumption of isotropically oriented ellipsoid axes, no significant distinctions between the two alternatives could be observed.

4.2. *Model Fitting*

The experimental $T_1(\nu)$ and $T_1(\nu, \Delta)$ results were fitted to the illustrated model functions by both model simulations and by the nonlinear Levenberg-Marquardt optimization (Micromath SCIENTIST [49]) of the numerous model parameters P_i involved in (1)–(6). In the general case one has 2 parameters for LU, (2) or (3), 2 for TR, (4), 4 for SD, (5), and 3 or 6 for Rot, (6a) or (6b). A typical dispersion measurement at fixed temperature ϑ and sample orientation Δ provides about 30 T_1-ν data pairs, which can be multiplied by considering the temperature and angular dependences and making use of known relations for the variations $P_i(\vartheta, \Delta)$. Such a simultaneous fitting of related data sets considerably improves the parameter estimation. Nevertheless it was found by the correlation matrix of the parameter optimization procedure [27] that only the LU and TR mechanisms could be disentangled unambiguously, whereas the high-frequency relaxation SD and Rot allowed more than one parameter set for a good curve fit.

As the correlation coefficients [49] of the parameter sets A_{SD}, $\tau_{SD\perp}$, α, η_{SD} on the one side and A_{Rot}, $\tau_{R\perp}$, η_{Rot} on the other proved near 0.9 or even larger, A_{SD} and A_{Rot} were fixed to the best results obtained for DMPC ($A_{SD} = 3.4\ 10^7\ s^{-2}$, $A_{Rot} = 3.4\ 10^9\ s^{-2}$). Furthermore, the anisotropy ratios η_i were taken from estimations given in the literature for DMPC [23, 47, 50] ($\eta_{SD} = 0$, $\eta_{Rot} \geq 30$), and the jump width ratio α was assumed liquid-like ($\alpha \leq 0.02$) [39, 40]. So finally only 4 parameters are left for a superposition of the three

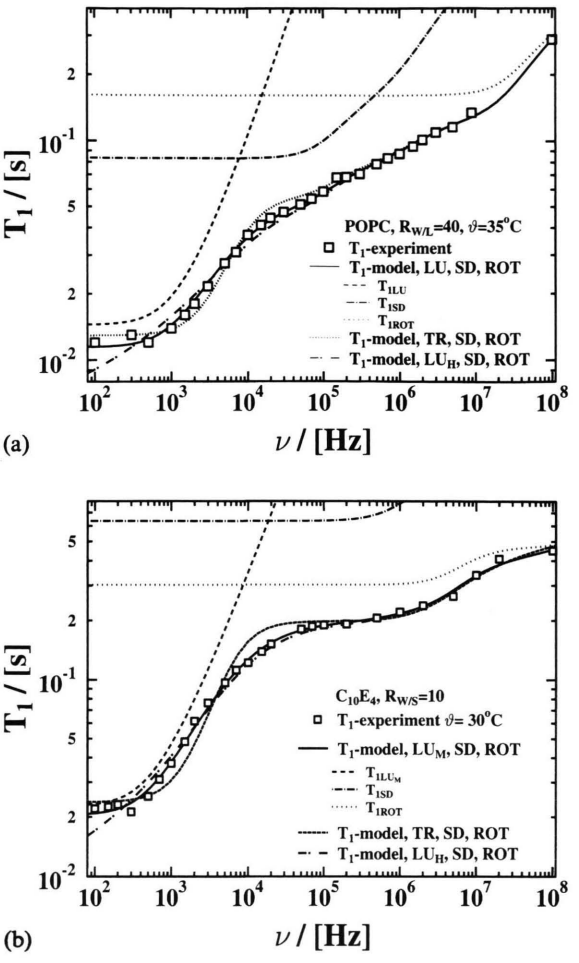

Fig. 7. Fits to the POPC system in the $L_\alpha + {}^2H_2O$-phase (a) and the surfactant system $C_{10}E_4$ in the L_α-phase (b) where the solid lines represent the best fit, using the linear dispersion law for the collective motion and an arctan cut-off behaviour. The various broken lines above the experimental data are the functions of the collective (LU) and the individual motions (SD and Rot), contributing to the overall relaxation. The two other fits of models using the TR-process in replacement of the LU-process (dotted line) and the logarithmic cut-off behaviour (Halle's simple coupling model) in the case of LU (dash dotted line) are added to compare the main differences. For these two additional fits we omitted drawing the functions of the underlying molecular motions.

model functions LU, SD and Rot *or* TR (RMTD), SD and Rot, respectively; whereas 6 parameters are involved if all four models, namely LU, TR (RMTD), SD and Rot, are taken into account for the curve fit.

The correlation coefficients R_{ij} (e.g. $A_{cu} - \tau_{SD}$) provide information on how closely estimates of the underlying parameters are depending on each other. Fol-

Table 2. Parameters evaluated in the last fitting step as described in text, using a nonlinear least squares fitting program. In the third section of the table, the cross correlation coefficients between the amplitude parameter of the collective motion A_{LU} and the correlation times of the individual motions and between the correlation times are listed. These factors were obtained by eliminating the ν_{cu} from the parameter estimation routine. In the last block of this table are parameters evaluated from fitting the model equations to the angular dependence of the T_1 dispersion measured for the oriented DMPC sample.

Lipids	$R_{W/L,S}$	ϑ °C	A_{LU} $10^5\ s^{-2}$	ν_{cl} kHz	τ_{SD} ns	τ_{Rot} ns
			Non oriented samples			
DMPC	15	30	4.5±0.27	2	47	68
DMPC	15	50	4.5±0.15	2.5	23	49
DMPC	40	35	14.5±0.3	1.6	19.2	10.6
DPPC	20	50	6.3±0.15	2.3	15	10.1
POPC	40	35	5.3±0.31	1.5	13	14
DOPC	40	35	2.9±0.16	4.4	16	27
DOPC	40	50	2.9±0.12	4.3	7.4	3.1
			Nonionic surfactants			
$C_{10}E_4$	10	30	1.5±0.03	0.6	7.0	81
$C_{12}E_3$	10	30	5.0±0.12	1.0	2.1	62
$C_{12}E_4$	10	30	2.6±0.10	1.7	22.0	2
$C_{12}E_4$	40	30	5.4±0.12	1.0	22.0	2
			POPC–$C_{12}E_4$ mixtures			
$R_{S/L}$	$R_{W/L,S}$	ϑ	A_{LU}	ν_{cl}	τ_{SD}	τ_{Rot}
1	19	25	4.95±0.01	1.6	26	30
4	13	25	4.17±0.07	1.1	12	11
			Correlation coefficients			
Lipids	$R_{W/L}$	ϑ °C	$A_{LU}-\tau_{SD}$	$A_{LU}-\tau_{Rot}$	$\tau_{SD}-\tau_{Rot}$	
DMPC	40	35	−0.55	0.26	−0.72	
DMPC	15	30	−0.70	0.48	−0.82	
DMPC	15	50	−0.57	0.37	−0.84	
DPPC	20	50	−0.55	0.39	−0.90	
POPC	40	35	−0.56	0.36	−0.80	
DOPC	40	35	−0.67	0.45	−0.81	
			Oriented sample			
Lipids	$R_{W/L}$	ϑ °C	A_{LU} $10^5\ s^{-2}$	ν_{cl} kHz	A_{SD} $10^7\ s^{-2}$	τ_{SD} ns	A_{Rot} $10^9\ s^{-2}$	τ_{Rot} ns	η_{Rot}
DMPC	11	45	5.6±0.36	2.5	5.8	7.3	2.5	106	50

lowing the definition of MicroMath [49] the R_{ij} are obtained from the normalization of the variance-covariance matrix **P** of the parameter set **X**, $\mathrm{cov}(\mathbf{X}) = \mathbf{P} = (\mathbf{J}^T\mathbf{J})^{-1}\sigma^2$, by $R_{ij} = P_{ij}/(P_{ii}P_{jj})^{1/2}$. σ is the standard deviation of the data and **J** is the Jacobian matrix of the minimization problem [49].

Figures 7 a/b illustrate typical curve fits for the *non-oriented* lipid POPC and surfactant $C_{10}E_4$ using LU-SD-Rot or TR-SD-Rot combinations. The related complete sets of optimized parameters, including selected correlation coefficients R_{ij}, are listed in Table 2. In agreement with the earlier studies of Rommel et al. [12], the diagrams clearly demonstrate that LU and TR are low-frequency relaxation processes whereas SD and Rot dominate the high-frequency dispersion. Marqusee's model LU_M, (2), is more adequate than Halles approach LU_H, (3), since the logarithmic profile fails to describe the strong observed $T_1(\nu)$ curvature at low ν's. However, extending (3) formally by a low-frequency cut-off ν_{CL}, i.e. replacing ν in (3) by $\nu_{eff} \equiv (\nu^2 + \nu_{CL}^2)^{1/2}$, gives as good results as Marqusee's relation. Two essential new results are that, compared

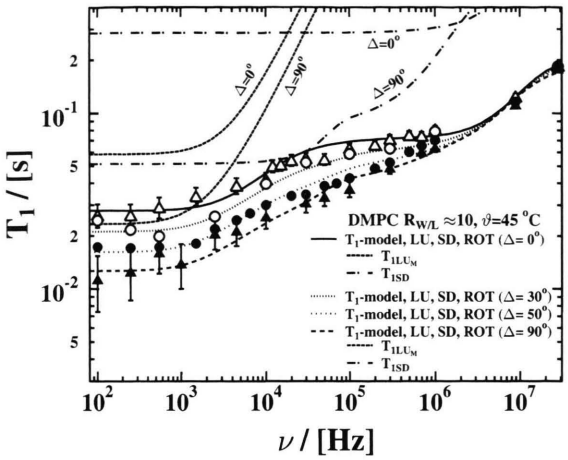

Fig. 8. The fit to the $T_1(\nu, \Delta)$ of the oriented DMPC system in the L_α-phase for the four orientations $\Delta = 0°$, 30°, 50° and 90°. As the filling factor for such samples is relatively poor, the error exceeds the symbol size in the low frequency range. The error bars for the 30 and 50° data were omitted for better clarity. The functions of the LU and the SD contributions to the total relaxation are added for the parallel and perpendicular orientation, respectively, in order to illustrate their changing influence by angle variations to the total relaxation in the low frequency range. The little kink in the 90° function for the SD-process at approximately 200 kHz is caused by numerical problems and has neither physical meaning nor a serious influence on the parameter fitting.

with best fits for TR-SD-Rot combinations, i.e. replacing LU by TR, Marqusee's LU contribution in range I works significantly better than a TR mechanism, (4). It was found [27], by allowing for general LU-TR-SD-Rot superpositions, that the assumption of a non-negligible TR process always needed an additional major LU contribution, whereas the opposite approach entailed an almost vanishing influence of TR. This result is supported by the temperature dependent T_1 measurements: Assuming a dominating TR mechanism in range I yields, in contradiction to (4c), increasing correlation times $\tau_{TR}(\vartheta)$ at higher temperatures ϑ, though the inverse Arrhenius behaviour of $D_\perp(\vartheta)$ is well-confirmed in the literature [50, 51]. A similar conflict was observed for all samples, i.e. for the lipids, the surfactants, and also the mixtures. Extensive model discussions for all studied materials are given in [27].

The angular dependent data $T_1(\nu, \Delta)$ for the *oriented* DMPC sample (Fig. 8) further support the preference of the LU approach, since (4a) cannot describe the strong decrease of the relaxation time with increasing angles Δ. One should note that the curve fits in Fig. 8 reflect in range I for $\Delta \neq 0$ effects of both the LU_M and the SD process, (2) and (5), as a consequence of the special, logarithmic low-frequency $T^{(0)}(p\nu)$ increase in the case of two-dimensional diffusion [27, 44, 45], when the ratio $\eta_{SD} = D_{\|}/D_\perp$ is close to zero. Table 2 includes some optimized fit parameters obtained by these measurements.

4.3 Discussion and Conclusions

Having demonstrated that the LU and not the TR process dominates the T_1 dispersion in frequency range I, the measurements provide a novel means to determine the bending rigidity κ_c of lamellar systems. Bending undulations have frequently been studied by optical methods which analyze the shape fluctuations of large vesicles [21, 52]. The bending rigidity is a basic quantity for the collective properties of membranes and hence subject of numerous molecular theoretical models [22, 52]. Our novel NMR method is *not* restricted to the existence of vesicles and hence can be

Table 3. Using (2c), the obtained parameters A_{LU} and the measured second moments are listed in the third and forth column. The elastic constants were calculated and are listed in the fifth column as $\kappa_{c\,Marqusee}$. In the last column are the corrected bending rigidities, calculated, using the refined model of Halle with $\kappa_{c\,Halle} \approx 0.219\,\kappa_{c\,Marqusee}$.

	$R_{W/L}$	A_{LU} $10^5\,s^{-2}$	$\langle\Delta\nu^2\rangle$ $10^6\,s^{-2}$	$\kappa_{c\,Marqusee}$ 10^{-19} Nm	$\kappa_{c\,Halle}$ 10^{-19} Nm
			Lipids		
DMPC	40	14.5	110	3.9±0.8	1.15±0.24
DMPC	15	4.5	110	12.5±3.0	3.67±0.88
DPPC	20	6.3	42	3.5±0.7	1.03±0.21
POPC	10	2.5	76	15.0±3.9	4.41±1.15
POPC	40	5.3	76	7.5±1.9	2.20±0.56
DOPC	40	2.9	82	17.3±4.5	5.08±1.32
			Surfactants		
$C_{12}E_3$	10	5.01	26.5	2.73±0.47	0.80±0.14
$C_{12}E_4$	10	2.64	20.3	3.96±0.74	1.17±0.22
$C_{12}E_4$	40	5.38	20.3	1.95±0.33	0.57±0.09
$C_{12}E_5$	10	1.28	14.5	5.81±1.01	1.71±0.30
$C_{12}E_6$	10	0.32	7.0	11.32±2.02	3.33±0.59
$C_{10}E_4$	10	1.54	12.2	4.06±0.69	1.19±0.20
$C_{16}E_4$	10	1.10	47.5	23.0 ±3.91	6.76±1.15
			POPC–$C_{12}E_4$ Mixtures		
$R_{S/L}$	$R_{W/(S+L)}$				
1	7	4.74	57.2	6.22±1.79	1.83±0.53
1	19	4.95	57.2	5.96±1.20	1.75±0.35
1	42	5.68	48.6	4.27±0.85	1.26±0.25
4	5	3.07	38.6	6.49±1.74	1.91±0.51
4	13	4.17	38.6	4.78±0.86	1.41±0.25
4	31	4.80	35.1	3.77±0.68	1.11±0.20

applied independently on the amount of water in the lipid systems and on surfactant bilayers or surfactant-water mixtures, where this optical method cannot be used. In order to extract κ_c from A_{LU}, the 2nd moment M_2 of the proton line must be known. Since the standard integration over the line shape [40] of unoriented lipids gives wrong results due to the existence of a super-Lorentzian component [53], the motionally averaged value $\langle M_2 \rangle$ was evaluated from the Jeener echo following the procedure of Bloom et al. [36]. We also estimated $\langle M_2 \rangle$ theoretically from the order of the proton pairs in the chain where such data were available in the literature [15, 27]. Table 3 summarizes $\langle M_2 \rangle$ and the related elasticity moduli κ_c obtained in this way by means of (2c) for all studied lipids, surfactants and mixtures for both models, including the uncoupled and the coupled layer undulations (with the assumption that a local field cut off and not an undulation mode cut off determines the low frequency behaviour; such local field cut off has already been discussed elsewhere [27, 38]. The theory for relaxation in such low fields is poorly developed and the spin temperature concept (M. Goldman) [54] used so far gives unsatisfying results [27, 38]. It seems that both the increasing density of multiple Larmor frequency states $n\nu$, with $n = 1, 2, 3, \ldots$ and the strength of local interactions (e.g. dipolar or quadrupolar) are important to describe the spin relaxation in low fields correctly).

It is seen that κ_c systematically varies as a function of water content, chain length and chain geometry: κ_c strongly increases both with decreasing amount of water and with increasing length of the saturated fatty acids; for comparable water content the lipids show slightly smaller values than the surfactants. Some typical variations are the increase of κ_c with the number of carbons in the alkyl-chain (lipids, surfactants) and in the headgroup (surfactants) of the membranes. The κ_c's evaluated by Marqusee's model, (2), are generally much higher, up to factors of 2–20, than results reported in the literature [21] for vesicles. These large deviations do *not* disappear if Halle's model, (3), i.e. his original concept in the fast diffusion limit, is used. They may on the one hand indicate distinctions between the different experimental techniques and error limits, but on the other side also the validity limits of Marqusee's model. However, Halle's recent approach [16] for the slow diffusion limit can reduce or even eliminate the deviations at least in the linear dispersion regime through the modified meaning of A_{LU}, namely $A^*_{LU} \cong 3.4\, A_{LU}$. But one should observe that a satisfactory application of Halle's new model needs refinements concerning the curvature of the $T_1(\nu)$ profile at low-frequencies, where in the present from the deviations of (3) and it's extension [16] from the experimental data (see Figs. 2–5) are obvious, except for DOPC (Fig. 2), essentially due to the absent mode cut-off (see Figure 8). In contrast to this result, (2a) describes all dispersion profiles quantitatively with ν_{CL} near 1 kHz, though the origin of the frequency cut-off ν_{CL} and the only minor variations between the various membrane systems (Table 2) is still not clear. Similar cut-offs were found in many nematic and smectic liquid crystals [8, 38]; most likely they must be attributed to internal local dipolar magnetic fields at the proton spin sites and not to a maximum coherence length.

Finally it should be mentioned that recently published results from measurements of T_{2eff} [55] gave values of κ_c very similar to those reported here. However, κ_c was obtained from the simple two dimensional LU theory which neglects membrane coupling. This may be fortuitous considering the different underlying theories. Anyway, a more detailed analysis of such experiments discussing the CMT theory, the underlying data analysis and the parameter analysis would be helpful.

The evaluated variations of κ_C essentially confirm predictions from Szleifer et al. [22] for simple ionic surfactants (single alkyl chains with an ionic headgroup). A more qualitative extrapolation of their results to lipids yields values which are in accordance with our data, whereas experimental results from Niggemann et al. [21] show considerably smaller values. However, both the hydration dependence and $R_{S/L}$ dependence of the mixtures agree with yet unpublished estimations of Galle [56], evaluated on the basis of Kozlovs theory on hexagonal lyotropic phases [57].

Acknowledgements

The authors thank Dipl. Phys. M. Krauß for his help in the experimental work and Dr. Pedro Sebastiao for calculating the spectral densities of the 2 dimensional translational selfdiffusion. Dr. H. Gotzig was involved in some instrumental developments. The authors also acknowledge the helps of Prof. G. Kothe, Dr. G. Althoff, and Dr. R. S. Prosser and the financial support by the Deutsche Forschungsgemeinschaft, SFB 294 Leipzig.

[1] P. G. de Gennes, The Physics of Liquid Crystals; Clarendon Press, Oxford 1974.
[2] M. F. Brown, J. F. Ellena, C. Trindle, and G. D. Williams, J. Chem. Phys. **84,** 465 (1986).
[3] P. I. Watnick, P. Dea, A. Nayeem, and S. I. Chan, J. Chem. Phys. **86,** 5789 (1987).
[4] R. Blinc, M. Luzar, M. Vilfan, and M. J. Burgar, J. Chem. Phys. **63,** 3445 (1975).
[5] J. A. Marqusee, M. Warner, and K. A. Dill, J. Chem. Phys. **81,** 6404 (1984).
[6] B. Halle, Phys. Rev. E **50,** R 2415 (1994).
[7] W. Wölfel, F. Noack, and M. Stohrer, Z. Naturforsch. **30a,** 437 (1975).
[8] F. Noack, M. Notter, and W. Weiss, Liq. Cryst. **3,** 907 (1988).
[9] M. Bloom and T. M. Bayerl, Can. J. Phys. **73,** 687 (1995).
[10] E. Blinc, D. Hogenboom, D. O'Reilly, and E. Petersen, Phys. Rev. Lett. **23,** 969 (1969).
[11] M. Vilfan, M. Kogoj, and R. Blinc, J. Chem. Phys. **86,** 1055 (1987).
[12] E. Rommel, F. Noack, P. Meier, and G. Kothe, J. Phys. Chem. **92,** 2981 (1988).
[13] W. Kühner, E. Rommel, F. Noack, and P. Meier, Z. Naturforsch. **42a,** 127 (1987).
[14] H. Bender, F. Noack, M. Vilfan, and R. Blinc, Liq. Cryst. **5,** 1233 (1989).
[15] J. Stohrer, G. Gröbner, D. Reimer, K. Weisz, C. Mayer, and G. Kothe, J. Chem. Phys. **95,** 672 (1991).
[16] B. Halle and St. Gustafsson, Phys. Rev. E **56,** 960 (1997).
[17] M. Bloom and E. Sternin, Biochemistry **26,** 2101 (1987).
[18] R. Kimmich and H. W. Weber, Phys. Rev. B **47,** 11788 (1993).
[19] G. Klose, St. Eisenblätter, J. Galle, A. Islamov, and U. Dietrich, Langmuir **11,** 2889 (1995).
[20] G. Klose, St. Eisenblätter, and B. König, J. Colloid Interface Sci. **172,** 438 (1995).
[21] G. Niggemann, M. Kummrow, and W. Helfrich, J. Phys. II France **5,** 413 (1995).
[22] I. Szleifer, D. Kramer, A. Ben-Shaul, W. Gelbart, and S. Safran, J. Chem. Phys. **92,** 6800 (1990).
[23] D. March, CRC Handbook of Lipid Bilayers; CRC Press, Boston 1990.
[24] G. Klose, B. König, and F. Paltauf, Chem. Phys. Lipids **61,** 265 (1992).
[25] F. Volke, St. Eisenblätter, J. Galle, and G. Klose, Chem. Phys. Lipids **70,** 121 (1994).
[26] N. J. Heaton, G. Althoff, and G. Kothe, J. Phys. Chem. **100,** 4944 (1996).
[27] J. Struppe, Thesis, Universität Stuttgart 1996.
[28] O. G. Mouritsen, Chem. Phys. Lipids **57,** 178 (1991).
[29] G. Klose, St. Eisenblätter, and B. König, J. Colloid and Interf. Science **172,** 438 (1995).
[30] B. König, PhD Thesis, Universität Leipzig 1993.
[31] L. Powers and N. A. Clark, Proc. Nat. Acad. Sci. **72,** 840 (1975).
[32] R. S. Prosser, S. A. Hunt, and R. R. Vold, J. Magn. Res. **B109,** 109 (1995).
[33] G. Klose, B. König, H. W. Meyer, G. Schulze, and G. Degovics, Chem. Phys. Lipids **47,** 225 (1988).
[34] C. Morrison, Biophys. J. **64,** 1063 (1993).
[35] F. Noack, St. Becker, and J. Struppe, Annual Reports on NMR Spectroscopy. Academic Press, London 1996 (in press).
[36] M. Bloom, E. E. Burnell, S. B. W. Roeder, and M. I. Valic, J. Chem. Phys. **66,** 3012 (1977).
[37] J. Struppe and F. Noack, 22. Freiburger Arbeitstagung, 15 (1993).
[38] J. Struppe and F. Noack, Liq. Cryst. **20,** 595 (1996).
[39] R. Y. Dong, Nuclear Magnetic Resonance of Liquid Crystals; Springer-Verlag, Heidelberg 1994.
[40] A. Abragam, The Principles of Nuclear Magnetic Resonance; Clarendon Press, Oxford 1970.
[41] J. H. Freed, J. Chem. Phys. **66,** 4183 (1976).
[42] S. Žumer and M. Vilfan, J. Physique **46,** 1763 (1985).
[43] R. Kimmich, W. Nusser, and T. Gneiting, Colloids and Surf. **45,** 283 (1990).
[44] M. Vilfan and S. Žumer, Phys. Rev. A **21,** 672 (1980).
[45] P. Sebastião, Thesis, University Lisbon 1993.
[46] H. C. Torrey, Phys. Rev. **92,** 962 (1961).
[47] P. L. Nordio, G. Rigatti, and U. Segre, J. Chem. Phys. **56,** 2117 (1972).
[48] D. E. Woessner, J. Chem. Phys. **37,** 647 (1962).
[49] Scientist Handbook; Micomath Inc., Salt Lake City 1995.
[50] P. Ukleja and J. W. Doane, in Ordering in Two Dimensions, Ed. S. K. Sinha, Elsevier, Amsterdam 1980; p. 427.
[51] P. Karakatsanis and Th. M. Bayerl. Phys. Rev. E **54,** 1785 (1996).
[52] S. König and E. Sackmann, Current Opinion in Colloid & Interface Science **1,** 78 (1996) and refs. given there.
[53] H. Wennerström and J. Ulmius, J. Magn. Res. **23,** 431 (1976).
[54] M. Goldman, Spin Temperature and Nuclear Magnetic Resonance in Solids, Pergamon Press, Oxford 1979.
[55] G. Althoff, N. J. Heaton, G. Gröbner, R. S. Prosser, and G. Kothe, Colloids and Surfaces A **115,** 31 (1996).
[56] J. Galle and G. Klose, in prep.
[57] M. M. Kozlov, S. Leikin, and R. P. Rand, Biophys. J. **67,** 1603 (1994).
[58] St. Gustafsson and B. Halle, J. Chem. Phys. **106,** 9337 (1997).